Available online at www.sciencedirect.com
ScienceDirect
Journal of Nuclear Materials 374 (2008) 461–472
journal of nuclear materials
www.elsevier.com/locate/jnucmat

In-pile Xe diffusion coefficient in UO_2 determined from the modeling of intragranular bubble growth and destruction under irradiation

K. Govers [a,b,*], S. Lemehov [b], M. Verwerft [b]

[a] Service de Métrologie Nucléaire (CP 165/84), Université Libre de Bruxelles, 50 Avenue F.D. Roosevelt, B-1050 Bruxelles, Belgium
[b] Institute of Nuclear Materials Science, SCK·CEN, Boeretang 200, B-2400 Mol, Belgium

Received 6 November 2006; accepted 26 October 2007

Abstract

Intragranular bubbles grow in the nuclear fuel by diffusion and precipitation of fission gases, mainly xenon; and are ultimately destroyed, under irradiation, by fission fragments. This article will attempt to determine the in-pile bubble distributions taking into account the evolution of the concentration profile around a bubble during its growth and the destruction process by fission fragments. From these distributions a relation between the bubble mean radius and the diffusion coefficient of xenon can be established, allowing the determination, from experimental measurements of intragranular bubble sizes, of the in-pile Xe diffusion coefficient in UO_2. The estimated activation energy (0.9 eV) is about one order of magnitude lower than the widely used value of 3.9 eV determined from out-of-pile experiments. This effect can be attributed to the presence of point defects created by the irradiation.

PACS: 61.72.Ji; 61.72.Qq; 61.80.−x; 66.10.Cb; 66.30.−h; 66.30.Jt

1. Introduction

Very recently Olander and Wongaswaeng [1] published the first part of a three-paper review of the different aspects of fission gas release (FGR). The first part reviews the irradiation induced fission gas resolution and the intragranular bubble distribution evolutions. The present article will focus on one specific aspect of intragranular gas behaviour: the in-pile lattice diffusion coefficient. Its derivation will be based on a careful modeling of intragranular bubble growth and the analysis of reported bubble size distributions (or bubble populations).

Intragranular bubbles were primarily studied to understand the role they play as temporary traps during the fission gas release process. This mechanism is generally modeled, see e.g. [1–7], distinguishing an effective diffusion coefficient from the single atom diffusion coefficient. The effective diffusion coefficient governs the macroscopic release rate and includes trapping and resolution effects, grain growth, bubble coalescence, etc. while the single atom diffusion coefficient describes the atomic-scale movement of individual gas atoms.

Together with the resolution mechanism, diffusion of individual atoms controls the formation, growth and destruction of intragranular bubbles. Although conceptually much simpler than the effective diffusion coefficient the determination of the single atom diffusion coefficient is not straightforward and persists to give rise to conflicting interpretations. The fundamental reason for this difficulty is the fact that one is interested in the in-pile value of this diffusion coefficient and that out-of-pile analysis techniques are not adapted for this determination. Only with a correct determination of the single atom in-pile diffusion coefficient can relevant calculations of the effective diffusion coefficient commence.

* Corresponding author. Address: Service de Métrologie Nucléaire (CP 165/84), Université Libre de Bruxelles, 50 Avenue F.D. Roosevelt, B-1050 Bruxelles, Belgium.
E-mail address: kgovers@sckcen.be (K. Govers).

0022-3115/$ - see front matter © 2007 Elsevier B.V. All rights reserved.
doi:10.1016/j.jnucmat.2007.10.005

One of the rare observables that is directly linked with this single atom diffusion coefficient is the size distribution of small (nanoscale) intragranular bubbles. Such bubbles have been observed by TEM techniques already for several decades, and several models have been proposed to describe their formation and growth.

In this paper, we will address some of the hypotheses that were used in earlier work and their validity will be assessed. A more thorough approach leads to somewhat more sophisticated expressions, but helps understand the domain of validity of certain hypotheses. We will finally derive the single atom in-pile diffusion coefficient from a set of published data.

For clarity purpose, the different symbols and notations used in this article are summarized in Table 1.

2. Theoretical and experimental background

2.1. Solution site and diffusion mechanism

A few studies have compared different solution sites energies for Xe atoms in the uranium dioxide matrix. These studies include *ab initio* [8,9], static calculations [10–13] and molecular dynamics simulations [14]. It appears from these works that the preferred solution site is either a di-vacancy ($V_U + V_O$) or a neutral tri-vacancy ($V_U + 2V_O$), depending on the chemical potential of the oxygen vacancy, which depends on the stoichiometry for out-of-pile analyses or on the irradiation conditions in in-pile experiments.

For the migration of one Xe atom a second uranium vacancy is needed according to the simulations of [10–

Table 1
Nomenclature

Name parameter	Definition	Typical value	Units
α_s	Fixed sink length	10^{15}	m^{-2}
b	Probability of destruction of a bubble (and of resolution of a Xe atom present in a bubble considering the model proposed in this article)	10^{-3}	s^{-1}
$C(r, t)$	Volumic concentration of Xe atoms in the lattice in r, at time t	10^{25}–10^{26}	(at.) m^{-3}
C_0	Volumic concentration of gas atoms in the matrix (lattice + intragranular bubbles)	10^{25}–10^{26}	(at.) m^{-3}
C_b	Volumic concentration of bubbles in the matrix	10^{23}–10^{24}	(bub.) m^{-3}
$C_{bub.}^{gas}$	Amount of gas atoms present in intragranular bubbles per matrix volume unit	–	(at.) m^{-3}
C_{lat}^{gas}	Amount of gas atoms present the lattice per matrix volume unit	–	(at.) m^{-3}
D_{eff}	Effective diffusion coefficient	10^{-17}–10^{-21}	m^2s^{-1}
D	In-pile diffusion coefficient of Xe atoms	10^{-17}–10^{-21}	m^2s^{-1}
D_i	$i = 1, 2, 3$ Partial contribution to the diffusion coefficient expression established by Turnbull [15]. Each term is dominant in a particular temperature range		m^2s^{-1}
$\dot{F}$	Fission rate	10^{18}–10^{19}	(fiss.) $m^{-3}s^{-1}$
$F(R_b, t)$	Flux of atoms at the surface of a bubble of radius R_b, at time t	–	(at.) s^{-1}
g	Probability per unit of time for a Xe atom to be trapped by a bubble	–	s^{-1}
j_v	Cation (uranium) vacancy jump rate: $j_v \approx \omega_D \exp(-2.4\ \text{eV}/k_B T)$		s^{-1}
K'	Rate of defect production per atom	10^4–5×10^5	(def.)/(fiss.)
k_B	Boltzmann constant	1.38×10^{-23}	$J\ K^{-1}$
λ	Adimensional parameter describing bubble growth in an infinite medium (see Section 4.2)	0–0.1	–
μ_{ff}	Length of a fission track	6–9	μm
$N_b(R_b)$	Number of gas atoms contained in a bubble of radius R_b	–	(at.)/(bub.)
ω_D	Debye frequency of the non-disturbed lattice	$\approx 10^{13}$	s^{-1}
Ω_{Xe}	Volume occupied by a gas atom inside an intragranular bubble	0.036	nm^3
P	Correction factor proposed by Lösönen expressing the probability of interaction of a fission fragment with a bubble at a distance lower than Z_0 from the track centerline	0–1	–
P_{des}	Probability of destruction of a bubble per unit of time, this value can depend or not on the bubble radius according to the chosen model		s^{-1}
$\overline{R_b}$	Bubble mean radius	0.5–...	nm
$R_b(t)$	Radius of the growing bubble at time t	–	nm
$R_{b,\tau}$	Radius of a bubble at time τ, it is an approximation of $\overline{R_b}$	–	nm
$\overline{R_b^3}$	Average of R_b^3 from the bubble population	–	nm^3
$\widetilde{R}_b$	Bubble most probable radius (peak value in the bubble distribution)	–	nm
R_{cv}	Radius of the capture volume	6–10	nm
$S(r, t)$	Volumic production rate of gas atoms in r, at time t	–	(at.)$m^{-3}s^{-1}$
T	Temperature	–	K
τ	Bubble mean lifetime. If the destruction process is independent of bubble size, $\tau = 1/b$	–	s
V	Vacancy concentration	–	(vac.)/(at.)
V_0	Thermodynamic concentration of vacancies: $\exp(-2.4\ \text{eV}/k_B T)$		(vac.)/(at.)
$\overline{V}$	Bubbles mean volume	–	nm^3
$V(R_b)$	Volume of a bubble of radius R_b: $V(R_b) = \frac{4\pi}{3} R_b^3$	–	nm^3
Z	Number of sites around a defect from which recombination is inevitable	100	
Z_0	Radius around the fission fragment path in which bubbles are entirely destroyed	7	nm

12]. Migration therefore occurs in a complex defect structure involving at least two uranium vacancies.

2.2. In-pile Xe diffusion coefficient

Different mechanisms influence the diffusion of fission gas atoms in the uranium dioxide matrix. Turnbull et al. [15] considers three main contributions, in three different temperature regimes. This description is now widely used by the scientific community concerned with fission gas behaviour in nuclear oxide fuels, see e.g. [5,6,16,17]. According to [15], the single atom diffusion coefficient can be expressed as

$$D = D_1 + D_2 + D_3, \tag{1}$$

where D_1 represents the intrinsic diffusion coefficient, i.e. the diffusion assisted by thermally created defects (intrinsic defects). Turnbull used the results of Davies and Long [18]

$$D_1 = 7.6 \times 10^{-10} \exp\left(\frac{-3.0\ \text{eV}}{k_B T}\right)\ \text{m}^2\text{s}^{-1}. \tag{2}$$

This mechanism provides the major contribution to fission gas diffusion at high temperature (above about 1400 °C).

The second term shows a lower activation energy that the D_1 term because of the influence of a non-equilibrium (uranium) vacancy concentration induced by the irradiation. It dominates the atomic diffusion coefficient in the temperature range 800–1400 °C. According to [15], D_2 may be represented as

$$D_2 = s^2 j_v V, \tag{3}$$

where s is the atomic jump distance (3.86 Å), $j_v = \omega_D \exp(-2.4\ \text{eV}/k_B T)\ \text{s}^{-1}$ the (uranium) vacancy jump rate in the non-disturbed lattice, ω_D is the Debye frequency and V the (uranium) vacancy concentration. This description assumes that Xe atom migration is controlled by diffusion of U vacancies to sites in the vicinity of the Xe atoms. The concentration of vacancies created by the irradiation (vacancies/atom) has been estimated by Sharp [19] considering mutual recombination of vacancies and interstitials and the presence of sinks

$$V_{\text{irr}} = \frac{(\alpha_s s^2 + Z V_0)}{2Z}\left(\left(1 + \frac{4K'Z}{j_v(\alpha_s s^2 + Z V_0^2)^2}\right)^{1/2} - 1\right), \tag{4}$$

where α_s is the fixed sink strength, K' is the defect production rate per atom and Z the number of recombination sites around a point defect from which recombination is inevitable and V_0 is the thermodynamic concentration of vacancies per atoms (in the non-disturbed lattice): $V_0 \approx \exp(-2.4\ \text{eV}/k_B T)$. When mutual recombination is dominant and when the irradiation induced creation of defects is larger than the thermal creation of defects, the vacancy concentration (vacancies/atom) can be approximated by

$$V \approx V_{\text{irr}} \approx \sqrt{K'/j_v Z}. \tag{5}$$

The combination of Eqs. (3) and (5) provides

$$D_2 = \text{constant} \times \sqrt{\dot{F}} \exp\left(\frac{-1.2\ \text{eV}}{k_B T}\right), \tag{6}$$

where $\dot{F}$ is the fission rate.

The last term, D_3 is the irradiation induced diffusion coefficient. It does not depend on temperature and is proportional to fission rate

$$D_3 = A\dot{F}, \tag{7}$$

where the numerical value of A is $1.2 \times 10^{-39}\ \text{m}^5$ for oxide fuels. This mechanism provides the major contribution to diffusion below 800 °C.

By analyzing intragranular bubble growth from TEM observations, one is capable of deriving an atomic-scale diffusion coefficient, which is the subject of this paper. A priori, our approach does not distinguish between diffusion mechanisms, but the data sets that are analyzed in this paper are situated in the temperature domain where the D_2 term is dominant, which is indeed the most important temperature domain for thermal fission gas release in LWR fuels.

2.3. Bubble observations

Intragranular bubble distributions have been extensively studied in the 1970s. Diffusion coefficient was, at that time, often derived from bubble growth after annealing at elevated temperature (e.g. [20]). Only a few articles [3,21–24] focused on the observation of intragranular bubbles just after irradiation. These data will enable the determination of an in-pile value for the diffusion coefficient of Xe. The irradiation conditions pertaining to the analyzed data are summarized in Tables 2 and 3.

Cornell [3,21] reports measurements made on four rods (A–D), irradiated under different conditions. These measurements were done at different distances from the pellet center, providing mean bubble radii at different temperatures under the same irradiation conditions. Baker [22] did the same for four (1–4) other rods, but measurements of mean radii are only reported in this article for the two first pins.

It is to be noted that these authors only report the mean value of the bubble size distribution found at each radial location. A bubble size distribution at each temperature was reported by Wood [24]. Unfortunately this pin showed columnar grains indicating that high temperature had been reached in the central zone of the pellet, resulting in a high fission gas release from these grains. The exact quantity of gas present in the grain was not reported by Wood (only an estimation of the produced amount), making it impossible to obtain quantitative results. However, these data do enable a qualitative validation of our approach, because, as it will be shown in this article, the theoretical shape of

Table 2
Characteristics of Cornell data

Specimen	Temperature (°C)	Fission rate (10^{18} m^{-3} s^{-1})	Burnup (MWd/kg$_U$)	C_{gas}^{latt}[a] (10^{24} m^{-3})	C_b (10^{24} m^{-3})	Observed mean diam. (nm)	Corrected[b] mean diam. (nm)	$\overline{R}_b$ (nm)
A	860	6.8	1.1	10.6	0.38	1.7	/	/
A	980	6.8	1.1	11.6	0.35	1.8	/	/
A	1060	6.8	1.1	12.5	0.33	1.9	/	/
A	1270	6.8	1.1	12.5	0.29	2	/	/
A	1425	6.8	1.1	10.6	0.246	2	/	/
A	1470	6.8	1.1	11.7	0.183	2.3	0.95	0.475
A	1510	6.8	1.1	9.5	0.132	2.4	1.05	0.525
A	1570	6.8	1.1	11.2	0.124	2.6	1.25	0.625
A	1580	6.8	1.1	13.1	0.118	2.8	1.45	0.725
B	785	2.6	6	50	0.33	1.6	/	/
B	870	2.6	6	50	0.3	1.9	/	/
B	900	2.6	6	50	0.29	2.1	0.72	0.36
C	775	2.59	12	100	0.34	1.7	/	/
C	825	2.59	12	100	0.32	1.8	/	/
C	850	2.59	12	100	0.3	1.9	/	/
C	860	2.59	12	100	0.29	2	/	/
C	875	2.59	12	100	0.27	2.1	0.72	0.36
C	880	2.59	12	100	0.26	2.06	0.69	0.345
D	775	6.42	7	56	0.26	1.74	/	/
D	950	6.42	7	56	0.2	2.1	0.72	0.36
D	1075	6.42	7	56	0.15	2.5	1.15	0.575
D	1110	6.42	7	56	0.14	2.6	1.25	0.625
D	1200	6.42	7	56	0.12	2.7	1.35	0.675
D	1250	6.42	7	56	0.1	3.1	1.8	0.9

[a] Assumed to be the amount of gas produced during the irradiation.
[b] The observed diameters have been corrected according to Rühle [25]. Too small bubbles have been rejected from our study and are denoted with a /.

Table 3
Characteristics of Baker data

Specimen	Temperature (°C)	Fission rate (10^{18} m^{-3} s^{-1})	Burnup (MWd/kg$_U$)	C_{gas}^{latt}[a] (10^{24} m^{-3})	C_b (10^{24} m^{-3})	Observed mean diam. (nm)	Corrected[b] mean diam. (nm)	$\overline{R}_b$ (nm)
1	950	9.375	7	100	0.92	1.25	/	/
1	1100	9.375	7	100	0.7	1.5	0.9	0.45
1	1215	9.375	7	100	0.55	1.6	1	0.5
1	1350	9.375	7	100	0.43	1.75	1.1	0.55
2	1000	9.375	7	100	0.87	1.4	/	/
2	1185	9.375	7	100	0.8	1.5	0.9	0.45
2	1400	9.375	7	100	0.59	1.8	1.3	0.65
2	1550	9.375	7	100	0.53	2.1	1.85	0.925
2	1625	9.375	7	100	0.52	2.25	2.05	1.025
2	1650	9.375	7	100	0.44	2.1	1.85	0.925
2	1700	9.375	7	100	0.41	2.2	2	1
2	1750	9.375	7	100	0.45	2.3	2.1	1.05
2	1800	9.375	7	100	0.38	2.6	2.4	1.2
3	1575	9	7	95	0.1	0.76	/	/
3	1815	9	7	95	0.1	0.9	/	/
3	1930	9	7	95	0.1	1.82	1.3	0.65
3	1980	9	7	95	0.1	2.6	2.4	1.2

[a] Assumed to be the amount of gas produced during the irradiation.
[b] The observed diameters have been corrected according to Rühle [25]. Too small bubbles have been rejected from our study and are denoted with a /.

the bubble distribution can be deduced from the mean radius only. Regarding the samples of Cornell and Baker, for which the gas concentration in the grain was neither reported, we approximated the gas content of the sample by the amount of gas locally produced. Indeed we can reasonably assume observations were made in the inner parts of the grains and are therefore less influenced by fission gas release at the grain boundaries. This approximation can nevertheless be debated for samples irradiated for a long time at high temperatures.

Cornell [3,21] measured the radius from the center of the bubble to the center of the first dark fringe observed on TEM images in overfocussing conditions [22]. It was found later [25] that the inner radius of the first dark

fringe was a better estimation of actual bubble radius, but with still an overestimation for small bubbles. Baker [22] took the inner radius and corrected his data according to Rühle, but it seems an erroneous interpretation of the legend has been made. Therefore we corrected ourselves the bubble radius, as can be seen in Tables 2 and 3. As the contrast becomes very poor for the smallest bubbles, it was decided to work with bubbles whose diameter is greater than 0.7 nm.

The distribution of bubbles shows a pronounced peak, and it is not clear that Cornell and Baker report the most probable radius (i.e. the peak value) or if they made an average. In the last case, attention has to be paid because the larger bubbles, even if not numerous, can contribute significantly to the average. The study of Section 5 will show that moving from most probable to mean radius will only change the derived diffusion coefficient by a factor ≈1.5, and has no influence on activation energy.

3. Modeling the in-pile bubble distribution

3.1. Description of bubble behaviour from its nucleation to its elimination

The initial radius of the bubbles ($R_b(0) = R_0$), their lifetime and a relation between $R_b(t)$ and the number of atoms inside a bubble are the parameters that can be deduced from the modeling of the bubble 'life': their nucleation, the equation of state for the gas and their destruction.

3.1.1. Nucleation

It is generally accepted [5,6,15,16,22,26,27] that bubbles nucleate in the wake of fission spikes because many bubbles are found in randomly oriented straight lines [22]. Cornell and Turnbull [28] also report that gas can be knocked-out from pores and precipitates as bubbles – again in straight lines – up to 1000 Å away from these pores [28].

According to Turnbull [15,29] the fission fragment creates large quantities of vacancies which agglomerate and form a cavity. This cavity can trap very quickly a few gas atoms, creating the initial bubble. The minimal stable size is, according to Turnbull, of about 5 Å, corresponding to a bubble of 4–5 gas atoms according to the Van der Waals equation of state (used in Turnbull's model). More recent observations of Nogita and Une [31] suggest a higher density for Xe inside intragranular bubbles; changing this number of atoms to 9–15. Nelson [30] on his side proposed that a bubble containing only two atoms was already stable. In this study a value of zero will be taken for the initial size. It is not expected to modify considerably the results, particularly at high temperature, because bubbles reach quite rapidly such a size.

3.1.2. Bubble growth

In previous models [21,26,27,29] it was generally assumed that Xe obeys the Van der Waals equation of state and that the surface of bubbles was at equilibrium; i.e. the surface tension compensates the inner pressure. The equilibrium of the surface can be questioned but the amount of gas in a nanometric bubble is not sensitive to this since the Van der Waals equation of state for Xe predicts density to be limited to 2.6 g/cm^3 at high pressure. It corresponds to a volume of 0.081 nm^3 per Xe atom.

Since the publication of these models, experimental observations of intragranular bubbles [31–34] have shown that they contain Xe in a near-solid phase, at least for Xe-implanted samples at low temperatures (Garcia et al.) and in the outer region of UO_2 pellets (Nogita and Une). It implies bubbles under very high pressures, in the GPa range. They estimated the density of Xe in the bubbles to lie between 3 and 6 g/cm^3, which corresponds to a volume of 0.036–0.072 nm^3 per Xe atom. In addition to this, no dependence of the density with the bubble size could be observed from the measurements of Nogita and Une (for bubble diameters ranging from 4 to 10 nm). The volume of a Xe atom in an intragranular bubble is according to these results close to the volume of one UO_2 molecule, which implies for the bubble to accommodate only one uranium vacancy per additional Xe atom.

The actual mechanism of bubble growth is still an open question, mainly concerning the importance of the vacancy flow to the bubble surface or the emission of dislocation loops from the bubble surface in order to equilibrate the bubble inner pressure. However, since the gas density equals the compressibility limit and since the uranium vacancy needed for the bubble relaxation due to an additional Xe atom is brought together with the Xe atom (see Section 2.1), the distinction of the uranium vacancy flow or other bubble relaxation mechanisms are not relevant for nanometric bubble growth.

For these reasons, the flow of gas atoms to the bubble surface will be modeled in this work as a diffusion process of the gas present in the matrix (see Section 3.2.1), assuming that each Xe atom in the bubbles has a volume of 0.036 nm^3. One should, however, be aware that the same hypothesis does not hold for the growth of larger bubbles where the gas density does vary with bubble size and where other mechanisms are at play.

3.1.3. Destruction

Considering the data of Cornell [21] (annealing conditions) and of Baker [22] (in-pile conditions), it can be observed that, at identical temperature, intragranular bubbles grow to a bigger size after annealing than after irradiation. Therefore a mechanism operating under irradiation exists, that limits bubble growth or continuously destroys them. Two models have been envisaged in the literature. The model of Nelson [30] (called homogeneous model by Olander and Wongaswaeng [1]) which proposes that atoms are re-dissolved one by one into the matrix due to collisions with fission fragments. With such a model it is difficult to explain the apparition of a new population of bubbles in a few hours [36]. Such a model should, however, be applicable for larger bubbles. In the second model, proposed by

Turnbull et al. [29] (called heterogeneous model by Olander and Wongaswaeng [1]), bubbles are completely destroyed if they are traversed by a fission fragment. This model was later improved by Turnbull [4] assuming bubbles are destroyed if their center is within a radius $Z_0 + R_b$ (Z_0 is a constant and R_b bubble radius) around a fission fragment path. In this case the probability per unit of time that a bubble would be destroyed is

$$P_{des}(R_b) = 2\dot{F}\pi(Z_0 + R_b)^2\mu_{ff}, \tag{8}$$

the factor two stems from the fact that two fission fragments are emitted per fission, $\dot{F}$ is fission rate and μ_{ff} is the recoil length of the fission fragment.

Assuming that an equilibrium situation is reached, the number of destroyed bubbles is then equal to the number of bubbles created in the wake of the fission fragment. According to Turnbull's original model [29] (without the constant Z_0) the number of destroyed bubbles would lie between 4 and 10 per fission event, depending on the bubble concentration. According to observations this value is quite underestimated: Baker [22] could observe from 10 bubbles at low temperature up to 100 at elevated temperature.

Lösönen considers it not physically justified to include the dependence of the destruction rate on the small intragranular bubble radius [16]. He suggests to use only the constant Z_0 instead of $Z_0 + R_b$ and adds a correcting factor P expressing the probability of interaction of the fragment with the bubble. This expression will be used in this study, with a value of $Z_0 \approx 3.5$ nm [16]; and the probability per unit of time of destruction of a bubble will be referred as b

$$b = 2P\dot{F}\pi Z_0^2\mu_{ff}. \tag{9}$$

It will appear later that the exact value of b (and thus of P or Z_0) does not affect activation energy but only the prefactor of the Arrhénius form of the diffusion coefficient.

3.2. Review of existing intragranular bubble growth models

3.2.1. Diffusion driven growth

Bubble growth can be modeled as a diffusion process occurring in the volume around the bubbles. In order to simplify the problem, it is (generally implicitly, because of the reference to Ham's work [37]) assumed [5,16,21,26,27,29,37] that bubbles are spherical, homogeneously nucleated in the UO_2 matrix and start growing at the same time. This study is then, for symmetry reasons, reduced to the growth of one bubble in a cell (the 'capture volume') approximated by a sphere whose volume is equal to the inverse of the concentration of bubbles in the matrix (C_b). This model implicitly assumes that the presence of a 'new' bubble population does not affect the gas concentration profile around the existing growing bubble too much. This could be justified if one considers that a fission spike cannot create new bubbles near (less than a few nm from) an existing one without destroying it.

The diffusion equation in the capture volume can then be written for $R_b < r < R_{cv}$

$$\frac{\partial C(r,t)}{\partial t} = D\nabla^2 C(r,t) + S(r,t) = D\frac{1}{r}\frac{\partial^2(rC(r,t))}{\partial r^2} + S(r,t), \tag{10}$$

where r is the distance to the bubble center. $S(r,t)$ is the source term corresponding to the difference between the instantaneous gas production (due to fissions) and escape from the grains (FGR). The variations of the average gas concentration in a grain occurs on larger timescales than bubble growth; therefore $S(r,t)$ will be neglected from here. This kind of problem is known as 'moving boundary problem' or Stefan problem. The boundary conditions (BC) are, according to Ham's hypotheses [37]

$$\begin{cases} C(r,t) = 0, & \text{at } r = R_b(t), \\ \frac{\partial C(r,t)}{\partial r} = 0, & \text{at } r = R_{cv}, \end{cases} \tag{11}$$

and the initial concentration profile is assumed to be uniform in the capture volume. The solution of this problem provides the flux of atoms at the surface of the bubble, and knowing the equation of state of the gas in the bubble, its radius as a function of time can be calculated.

This problem has already been addressed by several authors [5,16,21,26,29] who used a relation for the flux established by Ham [37] under the assumption that bubble size is much smaller than the capture volume: $R_b \ll R_{cv}$. Note that in the case of intragranular bubbles, R_b varies from 0.5 to 1.5 nm and R_{cv} between 6 and 15 nm. Fortunately, at high temperature, when the bubble radii are bigger, the concentration of gas bubbles decreases [6,16,23], making this assumption more or less valid. Ham developed the solution in terms of the eigenfunctions of Eq. (10) subjected to the BC (11), and observed that only the first term contributed to the flux after a rapid transient (the ratio τ_1/τ_0 of decay constants associated to the second and first eigenfunction is about $0.15R_b/R_{cv} \ll 1$). The concentration profile was in that case

$$C(r,t) \approx C_0 e^{(-t/\tau_0)}\left(1 - \frac{R_b}{r} - \frac{1}{2}\frac{R_b r^2}{R_{cv}^3}\right), \tag{12}$$

with $\tau_0 = D\frac{3R_b}{R_{cv}^3}$, and the total flux at the bubble surface is

$$F(R_b,t) = 4\pi D C_0 e^{(-t/\tau_0)} R_b. \tag{13}$$

In this expression the terms $C_0 e^{(-t/\tau_0)}$ can be replaced by $C_0 - C_b N_b(R_b)$ to a good approximation since $0.15R_b/R_{cv} \ll 1$ and since matter is conserved. Finally the bubble growth rate can be calculated from the flux and the number of atoms present in the bubble

$$\frac{dN_b}{dt} = \frac{4\pi R_b^2}{\Omega_{Xe}}\frac{dR_b}{dt} = F(R_b,t), \tag{14}$$

therefore

$$\frac{dR_b}{dt} = D\frac{C_0\Omega_{Xe} - \left(\frac{R_b}{R_{cv}}\right)^3}{R_b}. \quad (15)$$

3.2.2. Diffusion coefficient from the saturation of bubbles

Approximate techniques allow to directly derive the diffusion coefficient from the Eqs. (13) or (15) of Section 3.2.1. One of these methods, used by Cornell in [21], assumes that saturation is reached. The amount of fission gas present in the matrix bubbles ($C_{bub}^{gas} = C_b\overline{N_b}$, where $\overline{N_b}$ is the average number of gas atoms per bubble), can then be related to the concentration of gas present in the lattice $C_{lat}^{gas} = C_0 - C_{bub}^{gas}$, by

$$gC_{lat}^{gas} = bC_{bub}^{gas}, \quad (16)$$

where b is the probability per second that a Xe atom in a bubble undergoes resolution (see Eq. (9)) and g is the probability that a Xe atom in the lattice is trapped by a bubble. Using Ham's results (Eq. (13)), g is equal to

$$g = 4\pi D\overline{R_b}C_b, \quad (17)$$

where $\overline{R_b}$ is the average radius of bubbles. From Eqs. (16) and (17)

$$D = \frac{b\overline{N_b}}{4\pi\overline{R_b}(C_0 - C_b\overline{N_b})}. \quad (18)$$

Cornell [21] described the gas in the bubble using the Van der Waals equation of state (which can now be questioned in light of the work of Nogita and Une [31], see Section 3.1.2). $\overline{N_b}$ was determined expressing the equilibrium of the bubble internal pressure with the surface tension. The equilibrium of the bubble is debatable but when the pressure is sufficiently high (in the GPa range) the Van der Waals equation of state reduces to a volume per atom independent of the pressure.

Cornell expressed the mean volume of the bubbles as $\overline{V} = \frac{4\pi}{3}\overline{R_b^3}$. This is in fact incorrect and should be replaced by $\overline{V} = \frac{4\pi}{3}\overline{R_b}^3$. Two experimental data are thus needed to use this relation (the bubble mean radius and the bubble mean volume), except if a relation can be found between bubble mean radius and bubble mean volume. In Section 5.3 we will establish that (Eq. (52))

$$\overline{V} = \frac{6}{\pi} \times \frac{4\pi\overline{R_b^3}}{3} = \frac{6}{\pi} \times V(\overline{R_b}). \quad (19)$$

Note that this method can also be used with Nelson's model [30] for resolution, adapting the expression for b.

3.2.3. Diffusion coefficient from the integration of bubble growth rate

Another method was used by Turnbull [29], based on the work of Ham [37], in order to determine diffusion coefficient from the bubble growth. When only a small fraction of the total gas is contained in intragranular bubbles, i.e.

$$\frac{R_b}{R_{cv}} \ll C_0\Omega_{Xe}. \quad (20)$$

Eq. (15) becomes

$$\frac{dR_b}{dt} = \frac{DC_0\Omega_{Xe}}{R_b}. \quad (21)$$

Approximating $\overline{R_b}$ by its value after the mean lifetime τ of a bubble: $R_{b,\tau}$

$$R_{b,\tau}^2 - R_0^2 = 2\Omega_{Xe}C_0D\tau. \quad (22)$$

In this article Turnbull [29] considered that the destruction of a bubble occurred if it interacted with a fission fragment (model of destruction with $Z_0 = 0$ and considering R_b). Noting that $\tau = 1/b$ and using Eq. (9), it leads to

$$D = \frac{\pi\dot{F}\mu_{ff}(R_{b,\tau}^4 - R_0^4)}{2\Omega_{Xe}C_0}. \quad (23)$$

Using the model of destruction chosen in this article (Eq. (9)); the solution is then

$$D = \frac{b\left(R_{b,\tau}^2 - R_0^2\right)}{2\Omega_{Xe}C_0} = \frac{\pi\dot{F}P\mu_{ff}Z_0^2\left(R_{b,\tau}^2 - R_0^2\right)}{\Omega_{Xe}C_0}. \quad (24)$$

This model only requires the experimental average radius of bubbles. It assumes that the fraction of total gas contained in the bubble is small. However no information is gained about the population of bubbles. A comparison of Eq. (42) to the solution developed in Section 4.2, Eq. (50), shows that the approximation $R_{\tau,b} \approx \overline{R}_b$ provides a diffusion coefficient correct to a factor $\pi/4 \approx 0.785$.

4. Improvement to the previous method

4.1. Avoiding the simplifications $R_b \ll R_{cv}$ and $C_bN_b \ll C_0$

A more rigorous calculation, avoiding the assumptions $R_b \ll R_{cv}$ and $C_bN_b \ll C_0$ can be presented as follows:

$$\begin{cases} \frac{\partial C}{\partial t} = D\nabla^2 C = D\frac{1}{r}\frac{\partial^2(rC)}{\partial r^2}, & \text{for } R_b < r < R_{cv}, \\ C(r,t) = 0, & \text{at } r = R_b, \\ \frac{\partial C(r,t)}{\partial r} = 0, & \text{at } r = R_{cv}, \\ C(r,t) = C_0, & \text{at } t = 0, \\ \frac{dR_b}{dt} = D\Omega_{Xe}\cdot\frac{\partial C}{\partial r}. \end{cases} \quad (25)$$

The solution can be expanded in terms of the eigenfunctions of the problem

$$C(r,t) = \sum_{k=0}^{\infty} C_k \frac{\sin\left(\sqrt{\alpha_k}(r - R_b)\right)}{r} e^{-\alpha_k Dt}, \quad (26)$$

where C_k are constants and α_k is a solution of

$$\tan\left(\sqrt{\alpha_k}(R_{cv} - R_b)\right) = R_{cv}\sqrt{\alpha_k}. \quad (27)$$

The lowest α_k, α_0 is developing $\tan(x) \approx x + \frac{x^3}{3}$

$$\alpha_0 = \frac{3R_b}{(R_{cv} - R_b)^3}. \quad (28)$$

The ratio of decay constants associated to the first and second eigenfunction is

$$\tau_1/\tau_0 = \alpha_0/\alpha_1 \approx 0.14\frac{R_b}{R_{cv}-R_b}.$$

Depending on the values of R_b and R_{cv} we know whether or not the higher harmonics can be considered as a 'rapid' transient. If this is not the case, the exact concentration profile around the bubble will greatly influence the results. In order to obtain an analytical relation between D and $\overline{R}_b$, we will assume that the fundamental mode is still sufficient to describe the growth process (i.e. $\tau_1/\tau_0 \ll 1$).

As the concentration profile depends on time only through the evolution of bubble radius, it can be expressed as

$$C(r,t) = X(R_b)\frac{\sin(\sqrt{\alpha_0}(r-R_b))}{r} \tag{29}$$

and $X(R_b)$ can be calculated expressing the conservation of the matter in capture volume and the bubble

$$X(R_b)\int_{R_b}^{R_{cv}}\frac{1}{r}\sin(\sqrt{\alpha_0}(r-R_b))4\pi r^2 dr = \frac{4\pi\left(C_0\Omega_{Xe}R_{cv}^3 - R_b^3\right)}{3\Omega_{Xe}}. \tag{30}$$

Thus, using $v = \frac{R_b}{R_{cv}}$,

$$C(R_b) = \frac{C_0\Omega_{Xe} - v^3}{\Omega_{Xe}R_b(1-v)\sqrt{1-v+3v^2-4v^3+v^4}}. \tag{31}$$

The factor $\sqrt{1-v+3v^2-4v^3+v^4}$ is almost constant and equal to 1 over a large range (up to $v \approx 0.7$ which will normally be satisfied for intragranular bubbles) and will thus be omitted from now. The growth rate can finally be expressed as

$$\frac{dR_b}{dt} = D\Omega_{Xe}\left.\frac{\partial C(r,t)}{\partial r}\right|_{r=R_b} = D\frac{C_0\Omega_{Xe} - \left(\frac{R_b^3}{R_{cv}^3}\right)}{R_b\left(1-\left(\frac{R_b}{R_{cv}}\right)\right)}. \tag{32}$$

Following the method presented in Section 3.2.3, we can obtain the diffusion coefficient by the integration of this expression. It gives, with the notation $\xi = \sqrt[3]{C_0\Omega_{Xe}}R_{cv}$

$$D = \left\{\frac{\ln\left(\frac{\left(\xi^3-R_{b,\tau}^3\right)(\xi-R_0)^3}{\left(\xi^3-R_0^3\right)(\xi-R_{b,\tau})^3}\right)}{6\xi} - \frac{\ln\left(\frac{\xi^3-R_{b,\tau}^3}{\xi^3-R_0^3}\right)}{3} - \frac{\left[\tan^{-1}\left(\frac{\xi+2R_{b,\tau}}{\sqrt{3}\xi}\right) - \tan^{-1}\left(\frac{\xi+2R_0}{\sqrt{3}\xi}\right)\right]}{\sqrt{3}\xi}\right\}\cdot\frac{R_{cv}^2}{\tau}. \tag{33}$$

4.2. Determination of the in-pile diffusion coefficient: infinite capture volume

In the two previous approaches, the transient due to the higher harmonics has been neglected. An exact analytical solution to the Stefan problem, can be obtained in the case of infinite matrix where the concentration of gas is uniform, assuming that each xenon atom occupies a fixed volume in the bubble. This volume will, as in the previous methods, be taken as the volume of xenon in a (near-)solid form. This problem is mathematically very similar to the solidification of a supercold liquid [38].

The main difference with the preceding approach is that now no conditions exist on the concentration gradient in R_{cv}, the local concentration at this point will decrease according to the developed solution without maintaining the condition of zero flux between cells. This condition appeared in the previous approach from the assumption that all bubbles nucleate at the same time, which is also unrealistic because the diameter of a fission track is smaller (7 nm) than the average distance between bubbles (14–20 nm). We do not expect the condition on the flux in R_{cv} to have a great influence on the results unless the losses of the gas in the capture volume is high. Eq. (10), the boundary and the initial conditions become, for an infinite capture volume

$$\begin{cases} \frac{\partial C}{\partial t} = D\nabla^2 C = D\frac{1}{r}\frac{\partial^2(rC)}{\partial r^2}, & \text{for } R_b < r < \infty \\ C(r,t) = 0, & \text{in } r = R_b \\ C(r,t) = C_0, & \text{for } r \to \infty \\ C(r,t) = C_0, & \text{at } t = 0 \\ \frac{dR_b}{dt} = D\Omega_{Xe}\cdot\frac{\partial C}{\partial r}. \end{cases} \tag{34}$$

By analogy to the 1D problem, a dependence in $\frac{r}{\sqrt{Dt}}$ is guessed. Then, with $s = \frac{r}{\sqrt{Dt}}$ the system (34) becomes

$$\frac{d^2C}{ds^2} = -\left(\frac{s}{2}+\frac{2}{s}\right)\frac{dC}{ds}. \tag{35}$$

Thus

$$C(s) = C_\infty + A\left[s\cdot e^{-\frac{s^2}{4}} - \frac{\sqrt{\pi}}{2}\mathrm{erfc}\left(\frac{s}{2}\right)\right], \tag{36}$$

and assuming that R_b varies as $R_b = 2\lambda\sqrt{Dt}$ the constant A is then given by

$$C(R_b,t) = 0 = C_0 + A\cdot\left(\frac{e^{-\lambda^2}}{2\lambda} - \frac{\sqrt{\pi}}{2}\mathrm{erfc}(\lambda)\right) \Rightarrow A = \frac{-C_0\cdot 2\lambda}{e^{-\lambda^2} - \lambda\sqrt{\pi}\mathrm{erfc}(\lambda)}. \tag{37}$$

The bubble growth rate is

$$\frac{dR_b}{dt} = 2\lambda^2\frac{D}{2\lambda\sqrt{Dt}} = \frac{2D\lambda^2}{R_b} = D\Omega_{Xe}\left.\frac{\partial C}{\partial r}\right|_{r=R_b} = D\Omega_{Xe}\frac{-C_\infty\cdot 2\lambda}{e^{-\lambda^2} - \lambda\sqrt{\pi}\mathrm{erfc}(\lambda)}\left[-\frac{e^{-\lambda^2}}{2\lambda R_b}\right]. \tag{38}$$

The parameter λ is thus the solution of

$$2\lambda^2\cdot e^{\lambda^2}\cdot\left(e^{-\lambda^2} - \lambda\sqrt{\pi}\mathrm{erfc}(\lambda)\right) = \Omega_{Xe}\cdot C_0. \tag{39}$$

The dependence of bubble radius is thus

$$R_b(t) = 2\lambda\sqrt{Dt}, \tag{40}$$

and the growth rate

$$\frac{dR_b}{dt} = \frac{2D\lambda^2}{R_b}. \quad (41)$$

This expression has the same form as Eq. (21). They become identical for very small values of λ as Eq. (39) reduces then to $\lambda^2 = C_0\Omega_{Xe}/2$. The same approximation ($R_{b,\tau} \approx \overline{R}_b$) can be made and, by analogy, the diffusion coefficient is given by (taking into account that in our model $R_0 = 0$)

$$D = \frac{b(R_{b,\tau}^2 - R_0^2)}{4\lambda^2} = \frac{bR_{b,\tau}^2}{4\lambda^2}. \quad (42)$$

5. Bubble size distribution

5.1. Determination of the bubble population

In the last section, we presented methods to express the diffusion coefficient as a function of the bubble mean radius. In the first approach (Section 3.2.2) a relation between bubble mean volume and bubble mean radius was needed, and in the other ones (Sections 3.2.3, 4, 4.2) we made the approximation: $R_{b,\tau} \approx \overline{R}_b$. We will now evaluate these approximations calculating explicitly the bubble population (i.e. the bubble size distribution). It will be based on the results obtained in the last approach (infinite capture volume), because it does not neglect the transient associated to the higher harmonics and because of the simplicity of the results it will provide.

Speight [26] already estimated the bubble population using the heterogeneous model for bubble destruction proposed by Turnbull [29]. The subsequent analysis is similar, but considering the correction proposed by Lösönen [16] for the destruction process.

If $C_b(R_b, t)dR_b$ is the concentration of bubbles with radii between R_b, $R_b + dR_b$, a conservation equation can be written

$$\frac{dC_b(R_b,t)}{dt} = \frac{\partial C_b(R_b,t)}{\partial t} + \frac{d}{dR_b}\left[C_b(R_b,t)\frac{dR_b}{dt}\right] = -P_{des}(R_b)C_b(R_b,t). \quad (43)$$

If the bubble population is at equilibrium, $\frac{\partial C_b(R_b,t)}{\partial t} = 0$ and this equation reduces

$$\frac{d}{dR_b}\left[C_b(R_b)\frac{dR_b}{dt}\right] = -P_{des}(R_b)C_b(R_b), \quad (44)$$

where $P_{des}(R_b)$ is defined in Eq. (8) and is equal to a constant (Eq. (9)) according to our hypothesis on bubble destruction. We decided to limit ourselves using only the bubble growth rate obtained in an infinite capture volume, Eq. (41), but Eqs. (41), (21) or (32) could also be used in the following developments.

The most probable radius $\widetilde{R}_b$ is the easiest value to deduce. It is obtained by setting $\frac{dC_b}{dR_b} = 0$ in (44), providing

$$\frac{d}{dR_b}\left(\frac{dR_b}{dt}\right) = -b. \quad (45)$$

Replacing $\frac{dR_b}{dt}$ by its expression (41), the diffusion coefficient is then given by

$$D = \frac{b\widetilde{R}_b^2}{2\lambda^2}. \quad (46)$$

From this expression it is clear that the conversion factor between radius and diffusion coefficient will just modify the prefactor of the Arrhénius expression of diffusion coefficient. The diameter of the fission spike will therefore not affect the conclusions on activation energy.

The bubble population is then obtained integrating Eq. (44). Using Eq. (41) for $\frac{dR_b}{dt}$ and normalizing this expression

$$\frac{C_b(R_b)}{C_b} = \frac{bR_b}{2D\lambda^2}e^{-b\frac{R_b^2}{4D\lambda^2}} = \frac{R_b}{\widetilde{R}_b^2}e^{-\frac{R_b^2}{2\widetilde{R}_b^2}}. \quad (47)$$

5.2. Relation between in-pile diffusion coefficient and bubble mean radius

The bubble mean radius $\overline{R}_b$ can be calculated, assuming a negligible initial size, from

$$\overline{R_b} = \frac{\int_0^\infty C(R_b)R_b dR_b}{\int_0^\infty C(R_b)dR_b}. \quad (48)$$

It leads to the relations

$$\overline{R_b} = \sqrt{\frac{\pi}{2}}\widetilde{R}_b \approx 1.253\widetilde{R}_b, \quad (49)$$

and finally

$$D = \frac{b\overline{R_b^2}}{\pi\lambda^2}. \quad (50)$$

A comparison of this result to Eq. (42) shows that the approximation $R_{b,\tau} \approx \overline{R_b}$ provides a diffusion coefficient correct to a factor $\pi/4 \approx 0.785$.

5.3. Bubble mean volume

The bubble mean volume $\overline{V}$ can be calculated from

$$\overline{V} = \frac{\int_0^\infty \frac{4\pi}{3}R_b^3 C(R_b)dR_b}{\int_0^\infty C(R_b)dR_b} = \frac{4\pi}{3}\cdot\frac{\int_0^\infty r^4 e^{-\frac{r^2}{2\widetilde{R}_b^2}}dr}{\int_0^\infty r e^{-\frac{r^2}{2\widetilde{R}_b^2}}dr} = \frac{4\pi}{3}\cdot\frac{3\sqrt{\pi}}{\sqrt{2}}\widetilde{R}_b^3 = \frac{6}{\pi}\cdot\frac{4\pi}{3}\overline{R}_b^3. \quad (51)$$

The radius corresponding to a bubble of mean volume $R_b(\overline{V})$ is thus equal to

$$R_b(\overline{V}) \approx 1.241\overline{R_b} \approx 1.555\widetilde{R}_b. \quad (52)$$

6. Deriving in-pile diffusion coefficient from observed bubble population

6.1. Results

The values of mean radius that can be found in Tables 2 and 3 were used to calculate the corresponding diffusion coefficient. The diffusion coefficient has been calculated with Eq. (50) which should provide the best estimate since the deficit of gas in the capture volume was low in each case. The transient associated to the higher harmonics cannot therefore be neglected. The values of D are plotted with a logarithmic scale as a function of $1/(k_B T)$ in Fig. 1. All sets of data tend to show the same activation energy, around 0.9 eV, and a prefactor $D_0 = (3.3 \pm 1.6) \times 10^{-12}$ cm^2/s.

From this study it not clear whether the prefactor is really different from one sample to the other because of the uncertainties on the experimental conditions and observation procedures. The prefactor can be proportional to $\sqrt{\dot{F}}$ as proposed in [15], but, e.g. a supplementary dependence on the gas concentration that would account for the number of vacancy sites per gas atom can not be excluded from our estimations. More experimental data are needed in order to address this issue. The in-pile diffusion coefficient reported by Turnbull [15], the out-of-pile diffusion coefficient determined by Cornell [20] and the diffusion coefficient in unirradiated material determined by Matzke [39] are also reported on the graph for comparison.

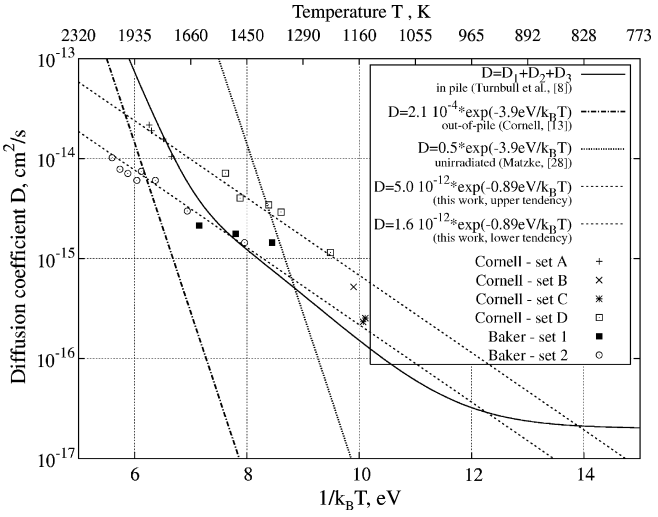

Fig. 1. Diffusion coefficient determined from bubble mean radii – comparison to Matzke [39], Cornell [20] and Turnbull [15]. Turnbull's curve is obtained considering a production of 5×10^5 defects per fission, and a fission rate of 10^{13} fiss./(cm^3 s).

6.2. Validation of the approach

The bubble distributions reported by Wood [24] will serve to assess the validity of the model. The mean radius was calculated from the experimental distribution. From this value the 'theoretical' bubble distribution was determined using Eq. (47), and compared to the experimental distribution in Figs. 2–5. It was chosen to calculate the theoretical shape from the mean radius (which is univoquely

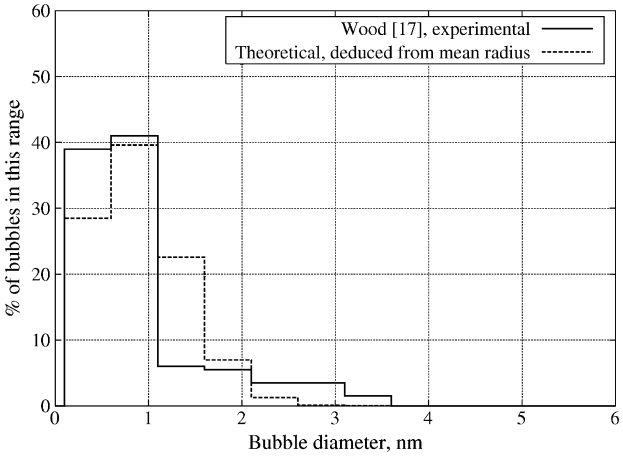

Fig. 3. Population of bubbles at 1815 °C.

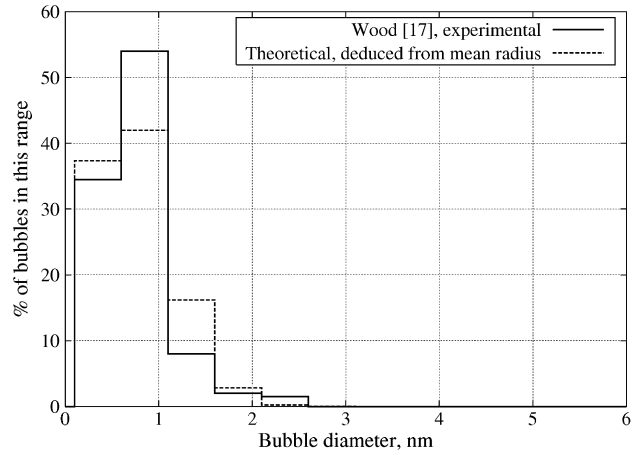

Fig. 2. Population of bubbles at 1575 °C.

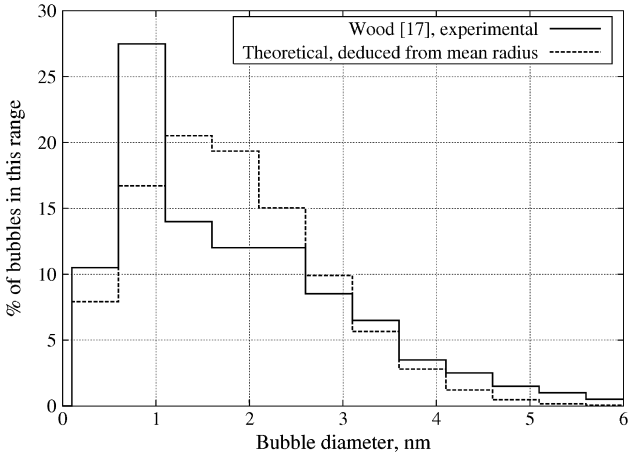

Fig. 4. Population of bubbles at 1930 °C.

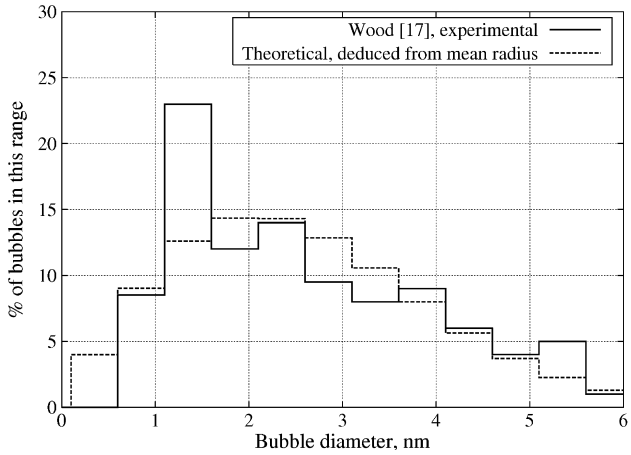

Fig. 5. Population of bubbles at 1980 °C.

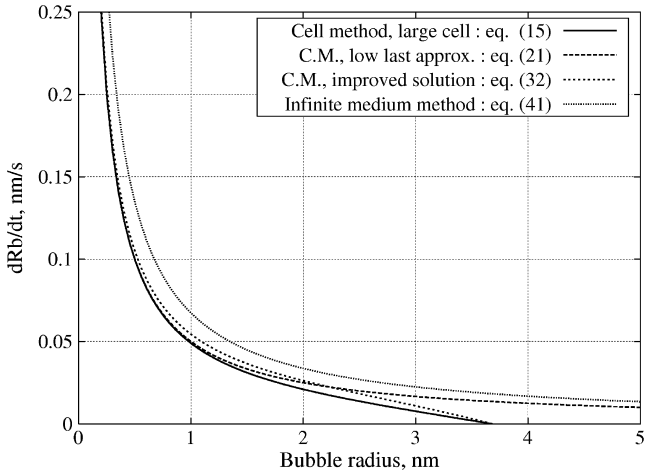

Fig. 6. Bubble growth rate as a function of bubble radius in this example, $D = 10^{-14}$ cm^2/s, $R_{cv} = 10$ nm and $C_0\Omega_{Xe} = 0.05$.

determined from the distribution) rather than fitting a function to the experimental distribution by varying the most probable radius (which is difficult to guess from the experimental graph). The plots of these functions in Figs. 2–5 present a good agreement, especially for the largest bubbles of the distribution. This means that the destruction probability for the biggest bubbles is well represented by our model and is thus independent of the bubble radius otherwise their size distribution would go faster to zero.

7. Discussion

The different above-mentioned methods have their own drawbacks and advantages. In the methods based on a cell description (Section 3.2) one considers that bubbles are much smaller than the capture volume, which in practice is more or less respected. We have proposed an improvement to this method (Section 4), that takes into account the finite size of the capture volume. Nevertheless, in order to obtain an analytical solution, we still have made the assumption that the transient associated with the higher harmonics is very rapid.

An analytical solution of the Stefan problem has been presented in the case of a bubble nucleating in an infinite matrix. This solution has the advantage that the transient is explicitly calculated, but the condition of zero flux at the surface of the capture volume is no longer maintained. This condition is debatable as the simultaneous nucleation of bubbles assumed in the other methods is also unrealistic. However, the condition on the concentration gradient in R_{cv} will not greatly influence the final solution, except in the case of large loss of the gas from the capture volume to the bubble.

A comparison of the bubble growth rate predicted by the different methods (Eq. (15); its approximation for low losses of gas in the capture volume, Eqs. (21), (32) and (41)) is plotted in Fig. 6. The curves are very close for small R_b but Eqs. (15) and (32) reaches zero when no more gas is present in the capture volume, as it was expected.

We will also compare the different prediction of diffusion coefficient by all these methods (Eqs. (18), (24), (33), (50)), using the same values for R_{cv} and $C_0\Omega_{Xe}$. This can be seen in Fig. 7. Again the agreement between the curves is good. The approach considering an infinite medium predicts the lowest diffusion coefficient because the transient associated to the higher harmonics is explicitly treated.

The general approach developed in this work was similar to that of Turnbull [29] and Speight [26], but with a different objective, that of determining the diffusion coefficient. The main difference is the hypothesis made regarding the destruction probability. In our work we consider that it is independent of bubble size, at least for the small intragranular bubbles. The activation energy we determined (0.9 eV) is similar to that estimated using Turnbull's approach [15] if mutual recombination dominate (1.2 eV); but it is much lower than the value calculated by Cornell [20] from out-of-pile experiment (≈3.9 eV), or than the widely used value of Matzke [39] (3.9 eV) obtained for unirradiated fuel. This is due to the fact that the defects needed for the diffusion are not in thermal equilibrium,

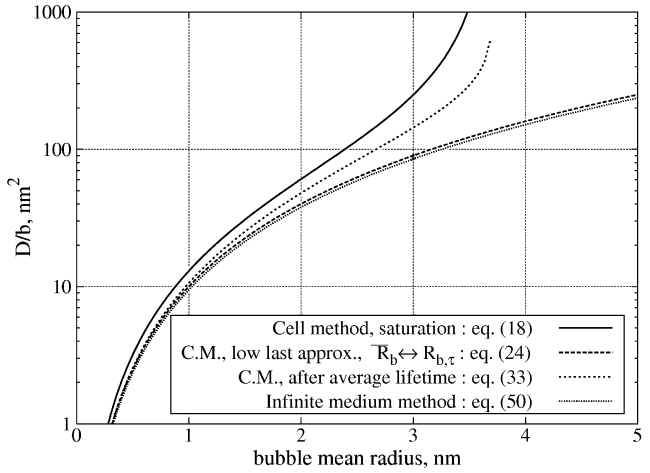

Fig. 7. Diffusion coefficient calculated with the different models in this example, $R_{cv} = 10$ nm and $C_0\Omega_{Xe} = 0.05$.

but rather that their concentration is regulated by the fission rate. The diffusion coefficient itself is lower, except at low temperature, than in the unirradiated material because of the presence of traps, but higher than in out-of-pile diffusion experiment on irradiated fuel, in agreement with the work of Matzke [40]. Interestingly, our results suggest that the diffusion process was the same over the whole temperature range considered (from 1100 to 2000 K), i.e. that the concentration of defects contributing to Xe diffusion is still controlled by the irradiation damages at 2000 K.

8. Conclusion

The model for bubble growth and destruction presented in this article provides a diffusion coefficient of the form $D \approx (3.3 \pm 1.6) \times 10^{-12} \exp(-0.9\ \mathrm{eV}/(k_B T))\ \mathrm{cm}^2/\mathrm{s}$ in the temperature range 1100–2000 K. The prefactor seems to be slightly sensitive to the fission rate (as suggested by Turnbull [15]), but a supplementary dependence on the concentration of gas in the lattice can not be excluded, which can be interpreted as the number of empty sites for diffusion per atom. More experimental data are required to confirm or infirm one of these hypotheses. The validity of the destruction model used in this article is confirmed by the bubble sizes distribution, especially for the largest bubbles because a different hypothesis on the destruction process would strongly modify the shape of this function at large bubble radii.

Acknowledgements

K.G. would like to thank Professor R. Beauwens (ULB) who was the promotor of his final year thesis on which this article is based, and SCK-CEN and ULB for his actual Ph.D. grant.

References

[1] D.R. Olander, D. Wongaswaeng, J. Nucl. Mater. 354 (2006) 94.
[2] M.V. Speight, Nucl. Sci. Eng. 37 (1969) 180.
[3] R.M. Cornell, M.V. Speight, B.C. Masters, J. Nucl. Mater. 30 (1969) 170.
[4] J.A. Turnbull, Radiat. Effect 53 (1980) 243.
[5] R.J. White, M.O. Tucker, J. Nucl. Mater. 118 (1983) 1.
[6] P. Lösönen, J. Nucl. Mater. 280 (2000) 56.
[7] K. Lassmann, H. Benk, J. Nucl. Mater. 280 (2000) 127.
[8] M. Freyss, N. Vergnet, T. Petit, J. Nucl. Mater. 352 (2006) 144.
[9] J.-P. Crocombette, J. Nucl. Mater. 305 (2002) 29.
[10] R.G.J. Ball, R.W. Grimes, J. Chem. Soc., Faraday Trans. 86 (1990) 1257.
[11] R.A. Jackson, C.R.A. Catlow, J. Nucl. Mater. 127 (1985) 161.
[12] C.R.A. Catlow, Proc. Roy. Soc. Lond. A 364 (1978) 473.
[13] S. Nicoll, Hj. Matzke, C.R.A. Catlow, J. Nucl. Mater. 226 (1995) 51.
[14] H.Y. Geng, Y. Chen, Y. Kaneta, M. Kinoshita, J. Alloy Compd., in press, doi:10.1016/j.jallcom.2007.03.030.
[15] J.A. Turnbull, C.A. Friskney, J.R. Findlay, F.A. Johnson, A.J. Walter, J. Nucl. Mater. 107 (1982) 168.
[16] P. Lösönen, J. Nucl. Mater. 304 (2002) 29.
[17] L.C. Bernard, J.L. Jacoud, P. Vesco, J. Nucl. Mater. 302 (2002) 125.
[18] D. Davies, G. Long, AERE Rep. No. 4347, 1963.
[19] J.V. Sharp, AERE Rep. No. 6267, 1969.
[20] R.M. Cornell, Philos. Mag. 19 (1969) 539.
[21] R.M. Cornell, J. Nucl. Mater. 38 (1971) 319.
[22] C. Baker, J. Nucl. Mater. 66 (1977) 283.
[23] C. Baker, J. Nucl. Mater. 71 (1977) 117.
[24] M.H. Wood, J. Nucl. Mater. 82 (1979) 257.
[25] M.R. Rüle. Proc. Conf. Radiation Induced Voids in Metals, 1971, p. 255.
[26] M.V. Speight, J. Nucl. Mater. 38 (1971) 236.
[27] Donald R. Olander, Fundamental Aspects of Nuclear Fuel Elements, Technical Information Center, Energy Research and Development Administration, 1976.
[28] R.M. Cornell, J.A. Turnbull, J. Nucl. Mater. 41 (1971) 87.
[29] J.A. Turnbull, J. Nucl. Mater. 38 (1971) 203.
[30] R.S. Nelson, J. Nucl. Mater. 31 (1969) 153.
[31] K. Nogita, K. Une, J. Nucl. Mater. 250 (1997) 244.
[32] K. Nogita, K. Une, Nucl. Instr. Meth., Phys. Res. B 141 (1998) 481.
[33] L.E. Thomas, L.A. Charlot, Nuclear waste management III, in: G.B. Mellinger (Ed.), Ceramic Transactions, vol. 9, The American Ceramic Society, 1990, p. 397.
[34] P. Garcia et al., J. Nucl. Mater. 352 (2006) 136.
[36] J.A. Turnbull, R.M. Cornell, J. Nucl. Mater. 41 (1971) 156.
[37] F.S. Ham, J. Phys. Chem. Solids 6 (1958) 335.
[38] John Crank, Free and Moving Boundary Problems, Oxford Science Publications, Clarendon Press, Oxford, UK, 1984.
[39] H. Matzke, in: I.J. Hastings (Ed.), Fission Product Behaviour in Ceramic Oxide Fuel, vol. 17, The American Ceramic society, 1986.
[40] H. Matzke, Radiat. Effect 53 (1980) 219.